Journal of Multidisciplinary Engineering Science and Technology (JMEST)
ISSN: 3159-0040
Vol. 2 Issue 10, October - 2015

Analytical Solutions To Elastic Functionally Graded Cylindrical And Spherical Pressure Vessels

Ahmet N. Eraslan
Department of Engineering Sciences
Middle East Technical University
Ankara 06531, Turkey
aeraslan@metu.edu.tr

Tolga Akis
Department of Civil Engineering
Atılım University
İncek, Ankara 06836, Turkey
tolga.akis@atilim.edu.tr

***Abstract*— Analytical solutions to earlier models by Chen and Lin [1] concerning elastic analysis of functionally graded cylindrical and spherical pressure vessels are obtained and presented.**

Keywords — Functionally graded materials; Elastic analysis; Thick cylinder; Spherical pressure vessel.

I. INTRODUCTION

Recently, Chen and Lin [1] have developed numerical models to investigate mechanical response of functionally graded cylindrical and spherical pressure vessels in the elastic state of stress. They have proposed that the modulus of elasticity E of the vessel vary radially according to

$$E(r) = E_0 \, exp\left[\frac{\beta(r-a)}{b-a}\right], \tag{1}$$

where E_0 is the value of E at the inner surface, r the radial coordinate, a and b the inner and outer radii, respectively, and β the grading parameter. Using basic equations of elasticity in cylindrical and spherical coordinates, they have obtained governing differential equations in terms of appropriately selected stress functions. These equations have then been solved numerically to obtain elastic behavior of the cylindrical and spherical vessels in turn subjected to either internal pressure or external pressure.

The governing equations as the outcome of the models by Chen and Lin [1] have both been second order, homogeneous, linear ordinary differential equations with variable coefficients. It is known that, although a little tedious, such equations can be solved analytically by power series method. In the present work accepting considerable help from the computer algebra systems Maple and Mathematica, analytical solutions to these equations are obtained. Meanwhile, the solution of a non-rotating annular disk is also obtained and presented in the Appendix Section.

The research on the prediction of stresses in basic mechanical structures like disks, cylinders, tubes, spherical shells, plates under different loading conditions has never ceased because of the importance of these structures in numerous civil, mechanical, electrical and computer engineering applications. In recent years extensive effort by researchers has also been spent for the mechanical analysis of basic structures made of functionally graded materials [1], [3]-[17]. A functionally graded material (FGM) is nonhomogeneous in its composition so that its properties like modulus of elasticity, modulus of rigidity, Poisson's ratio, and coefficient of thermal expansion may vary continuously throughout the material. This nonhomogeneity in the material may accompany lower stresses and as a result higher strength of the structure. The interested reader may acquire useful information on the subject matter from the list of most recent publications cited in this article.

II. FUNCTIONALLY GRADED CYLINDRICAL PRESSURE VESSEL

A. Formulation

The equation of equilibrium

$$\frac{d\sigma_r}{dr} + \frac{\sigma_r - \sigma_\theta}{r} = 0, \tag{2}$$

the compatibility relation

$$\frac{d}{dr}(r\epsilon_\theta) - \epsilon_r = 0, \tag{3}$$

the equations of generalized Hooke's Law

$$\epsilon_r = \frac{1}{E}[\sigma_r - \nu(\sigma_\theta + \sigma_z)], \tag{4}$$

$$\epsilon_\theta = \frac{1}{E}[\sigma_\theta - \nu(\sigma_r + \sigma_z)], \tag{5}$$

$$\epsilon_z = \frac{1}{E}[\sigma_z - \nu(\sigma_r + \sigma_\theta)], \tag{6}$$

form the basis for the solution [2]. In these equations σ_r, σ_θ and σ_z represent the normal stress components, ϵ_r, ϵ_θ and ϵ_z the normal strain components, and ν the Poisson's ratio. In case of plane strain, the axial strain vanishes, i.e. $\epsilon_z = 0$, and hence the axial stress is determined to be $\sigma_z = \nu(\sigma_r + \sigma_\theta)$. The radial and circumferential strains then take the forms

$$\epsilon_r = \frac{1-\nu^2}{E}\left[\sigma_r - \frac{\nu}{1-\nu}\sigma_\theta\right], \tag{7}$$

$$\epsilon_\theta = \frac{1-\nu^2}{E}\left[\sigma_\theta - \frac{\nu}{1-\nu}\sigma_r\right]. \tag{8}$$

Introducing a stress function of the form $F(r) = r\sigma_r$, one can write with the help of (2)

$$\sigma_r = \frac{F}{r}, \quad and \quad \sigma_\theta = \frac{dF}{dr}, \tag{9}$$

and as a result, the stress function F satisfies the equation of equilibrium. In terms of F, elastic strains can be rewritten as

$$\epsilon_r = \frac{1-\nu^2}{E}\left[\frac{F}{r} - \frac{\nu}{1-\nu}\frac{dF}{dr}\right], \tag{10}$$

$$\epsilon_\theta = \frac{1-\nu^2}{E}\left[\frac{dF}{dr} - \frac{\nu}{1-\nu}\frac{F}{r}\right]. \tag{11}$$

The governing differential equation in terms of $F(r)$ is obtained by substituting the strains from (10) and (11) into the compatibility equation. The result is

$$\frac{d^2F}{dr^2} + \frac{1}{r}\frac{dF}{dr} - \frac{F}{r^2} - \left(\frac{dF}{dr} - \frac{\nu}{1-\nu}\frac{F}{r}\right)\frac{1}{E}\frac{dE}{dr} = 0. \tag{12}$$

B. Analytical Solution

Note that with the form by (1) we determine

$$\frac{1}{E}\frac{dE}{dr} = \frac{\beta}{b-a}, \tag{13}$$

hence the governing equation takes the form

$$\frac{d^2F}{dr^2} + \frac{1}{r}\frac{dF}{dr} - \frac{F}{r^2} - \left(\frac{dF}{dr} - \frac{\nu}{1-\nu}\frac{F}{r}\right)\frac{\beta}{b-a} = 0, \tag{14}$$

or

$$\frac{d^2F}{dr^2} + \left(\frac{1}{r} - A\right)\frac{dF}{dr} - \left(\frac{1}{r} - B\right)\frac{F}{r} = 0, \tag{15}$$

where

$$A = \frac{\beta}{b-a}, \quad and \quad B = -A + \frac{\beta}{(b-a)(1-\nu)}. \tag{16}$$

This is a homogeneous second order linear differential equation with variable coefficients. Its analytical solution is obtained by power series method and can be displayed in the form

$$F(r) = C_1 P(r) + C_2 Q(r), \tag{17}$$

where C_1 and C_2 are arbitrary integration constants and the rest are

$$\begin{aligned} P(r) = r &+ \frac{\beta(1-2\nu)}{3(b-a)(1-\nu)}r^2 \\ &+ \frac{\beta^2(1-2\nu)(2-3\nu)}{24(b-a)^2(1-\nu)^2}r^3 \\ &+ \frac{\beta^3(1-2\nu)(2-3\nu)(3-4\nu)}{360(b-a)^3(1-\nu)^3}r^4 \\ &+ \frac{\beta^4(1-2\nu)(2-3\nu)(3-4\nu)(4-5\nu)}{8640(b-a)^4(1-\nu)^4}r^5 \\ &+ \frac{\beta^5(1-2\nu)(2-3\nu)(3-4\nu)(4-5\nu)(5-6\nu)}{302400(b-a)^5(1-\nu)^5}r^6 \\ &+ \cdots, \end{aligned} \tag{18}$$

$$Q(r) = P(r)\, I_t(r), \tag{19}$$

and

$$I_t(r) = \int_a^r \exp\left(\frac{\beta\lambda}{b-a}\right)\frac{d\lambda}{\lambda P(\lambda)^2}. \tag{20}$$

The series in (18) simplifies significantly if the Poisson's ratio is assigned to a numerical value. As an example, for $\nu = 3/10$ it simplifies to

$$\begin{aligned} P(r) &= r + \frac{4\beta}{21(b-a)}r^2 + \frac{11\beta^2}{294(b-a)^2}r^3 \\ &+ \frac{11\beta^3}{1715(b-a)^3}r^4 + \frac{55\beta^4}{57624(b-a)^4}r^5 \\ &+ \frac{44\beta^5}{352947(b-a)^5}r^6 + \cdots \end{aligned} \tag{21}$$

The rapid convergent nature of the solution can be observed here as $\nu \approx 3/10$ always.

The function $I_t(r)$ is determined by first expanding the integrand into MacLaurin's series and then performing the integration. For $\nu = 3/10$ first few terms of the result simplify to

$$\begin{aligned} I_t(r) &= \frac{1}{2}\left(\frac{r^2-a^2}{a^2r^2}\right) + \frac{13\beta}{21(b-a)}\left(\frac{r-a}{ar}\right) \\ &+ \frac{15\beta^2\ln(r/a)}{98(b-a)^2} + \frac{1157\beta^3(r-a)}{92610(b-a)^3} \\ &- \frac{20353\beta^4(r^2-a^2)}{15558480(b-a)^4} - \frac{326677\beta^5(r^3-a^3)}{1143548280(b-a)^5} \\ &- \frac{18791921\beta^6(r^4-a^4)}{960580555200(b-a)^6} \\ &+ \frac{56883671\beta^7(r^5-a^5)}{35301335403600(b-a)^7} + \cdots \end{aligned} \tag{22}$$

C. Evaluation of Integration Constants

In case of a cylinder subjected to internal pressure, P_{in}, the boundary conditions read $\sigma_r(a) = -P_{in}$, and $\sigma_r(b) = 0$, then the constants C_1 and C_2 are determined to be

$$C_1 = -\frac{aP_{in}Q(b)}{P(a)Q(b) - P(b)Q(a)} = -\frac{aP_{in}}{P(a)}, \tag{23}$$

$$C_2 = \frac{aP_{in}P(b)}{P(a)Q(b) - P(b)Q(a)} = \frac{aP_{in}P(b)}{P(a)Q(b)} \ , \qquad (24)$$

since $Q(a) = 0$ by (20). If the cylinder is subjected to external pressure, P_{ex}, boundary conditions become $\sigma_r(a) = 0$, and $\sigma_r(b) = -P_{ex}$, then the unknown constants turn out

$$C_1 = 0 \, , \quad C_2 = -\frac{bP_{ex}}{Q(b)} \ . \qquad (25)$$

III. FUNCTIONALLY GRADED SPHERICAL PRESSURE VESSEL

A. Formulation

The equation of equilibrium

$$\frac{d\sigma_r}{dr} + \frac{2(\sigma_r - \sigma_\theta)}{r} = 0, \qquad (26)$$

the compatibility relation given by (3) above and the equations of generalized Hooke's Law

$$\epsilon_r = \frac{1}{E}[\sigma_r - 2\nu\sigma_\theta], \qquad (27)$$

$$\epsilon_\theta = \frac{1}{E}[(1-\nu)\sigma_\theta - \nu\sigma_r], \qquad (28)$$

are the basic equations [2]. If we use a stress function of the form $F(r) = r^2\sigma_r$, then we find from the equation of equilibrium

$$\sigma_\theta = \frac{1}{2r}\frac{dF}{dr} \ , \qquad (29)$$

so that the equation of equilibrium is satisfied by $F(r)$ and meanwhile the elastic strains take the forms

$$\epsilon_r = \frac{1}{E}\left[\frac{F}{r^2} - \frac{\nu}{r}\frac{dF}{dr}\right], \qquad (30)$$

$$\epsilon_\theta = \frac{1}{E}\left[\frac{1-\nu}{2r}\frac{dF}{dr} - \nu\frac{F}{r^2}\right]. \qquad (31)$$

Substitution of elastic strains into the compatibility equation, (3), leads to the governing equation for the spherical vessel

$$\frac{d^2F}{dr^2} - \frac{2F}{r^2} - \left(\frac{dF}{dr} - \frac{2\nu}{1-\nu}\frac{F}{r}\right)\frac{1}{E}\frac{dE}{dr} = 0. \qquad (32)$$

Here we note the misprint in (28) of [1]. The term F/r^2 there should have been $2F/r^2$.

B. Analytical Solution

With the substitution of $\beta/(b-a)$ in place of $1/E \; dE/dr$ the governing equation becomes

$$\frac{d^2F}{dr^2} - \frac{2F}{r^2} - \left(\frac{dF}{dr} - \frac{2\nu}{1-\nu}\frac{F}{r}\right)\frac{\beta}{b-a} = 0. \qquad (33)$$

or after a rearrangement

$$\frac{d^2F}{dr^2} - A\frac{dF}{dr} - \left(\frac{1}{r} - B\right)\frac{2F}{r} = 0, \qquad (34)$$

where

$$A = \frac{\beta}{b-a} \ , \ and \ \ B = -A + \frac{\beta}{(b-a)(1-\nu)} \ . \qquad (35)$$

The power series solution of (34) can be cast into the compact form

$$F(r) = C_1P(r) + C_2Q(r), \qquad (36)$$

where

$$P(r) = r^2\left[1 + \frac{\beta(1-2\nu)}{2(b-a)(1-\nu)}r + \frac{\beta^2(1-2\nu)(3-5\nu)}{20(b-a)^2(1-\nu)^2}r^2 + \frac{\beta^3(1-2\nu)(2-3\nu)(3-5\nu)}{180(b-a)^3(1-\nu)^3}r^3 + \frac{\beta^4(1-2\nu)(2-3\nu)(3-5\nu)(5-7\nu)}{5040(b-a)^4(1-\nu)^4}r^4 + \frac{\beta^5(1-2\nu)(2-3\nu)(3-4\nu)(3-5\nu)(5-7\nu)}{100800(b-a)^5(1-\nu)^5}r^5 + \cdots\right], \qquad (37)$$

$$Q(r) = P(r)I_s(r), \qquad (38)$$

and

$$I_s(r) = \int_a^r \exp\left(\frac{\beta\lambda}{b-a}\right)\frac{d\lambda}{P(\lambda)^2} \ . \qquad (39)$$

Further simplification for $P(r)$ is possible upon substitution of numerical value for ν. The result for $\nu = 3/10$ is

$$P(r) = r^2\left[1 + \frac{2\beta}{7(b-a)}r + \frac{3\beta^2}{49(b-a)^2}r^2 + \frac{11\beta^3}{1029(b-a)^3}r^3 + \frac{319\beta^4}{201684(b-a)^4}r^4 + \frac{957\beta^5}{4705960(b-a)^5}r^5 + \cdots\right]. \qquad (40)$$

The integral $I_s(r)$ is determined as in the case of a cylinder.

C. Evaluation of Integration Constants

We note again that $Q(a) = 0$. When the vessel is subjected to internal pressure P_{in} the boundary conditions are $\sigma_r(a) = -P_{in}$, and $\sigma_r(b) = 0$. Accordingly the unknown constants are determined as

$$C_1 = -\frac{a^2P_{in}}{P(a)} \ , \quad C_2 = \frac{a^2P_{in}P(b)}{P(a)Q(b)} . \qquad (41)$$

In case of a vessel under external pressure boundary conditions read $\sigma_r(a) = 0$, and $\sigma_r(b) = -P_{ex}$, then the constants are evaluated as

$$C_1 = 0 \ , \quad C_2 = -\frac{b^2P_{ex}}{Q(b)} . \qquad (42)$$

IV. Presentation of Results

A. Cylindrical Pressure Vessel

In all of the following calculations $\nu = 3/10 = 0.3$. Furthermore, the results are presented in terms of the following dimensionless variables: radial coordinate

$$\bar{r} = \frac{r-a}{b-a} \quad , \tag{43}$$

radial stress component

$$\bar{\sigma}_r = -\frac{F}{rP_E} \quad , \tag{44}$$

and circumferential stress component

$$\bar{\sigma}_\theta = \frac{dF}{dr}\frac{1}{P_E} \quad , \tag{45}$$

where P_E represents either internal or external pressure. First, the pressure vessel with a relative wall thickness $a/b = 0.5$ which is subjected to internal pressure is considered. The dimensionless stresses are calculated for the values of the grading parameter β used in [1]. The results of these calculations are tabulated in Tables 1 and 2. In Table 1 analytical values of $\bar{\sigma}_r$ to 8-significant figures are tabulated clash with the numerical results of Chen and Lin [1], while Table 2 does the same for the results of $\bar{\sigma}_\theta$.

Using β as a parameter, calculations are also performed for a wall thickness of $a/b = 0.9$. The vessel is under internal pressure. The results of these calculations are depicted in Fig. 1 and Fig. 2. Fig. 1 shows the distributions of $\bar{\sigma}_r$ and Fig. 2 $\bar{\sigma}_\theta$ for different β values. In these figures dots come from the work of Chen and Lin [1] and represent numerical counterpart of the present solutions.

B. Spherical Pressure Vessel

In this case the nondimensional variables are

$$\bar{\sigma}_r = -\frac{F}{r^2P_E} \quad , \quad and \quad \bar{\sigma}_\theta = \frac{1}{2r}\frac{dF}{dr}\frac{1}{P_E} \quad . \tag{46}$$

A spherical pressure vessel of wall thickness $a/b = 0.5$ subjected to internal pressure is taken into consideration. Calculations are performed for different values of grading parameter β. The results of these calculations are plotted in Fig. 3 and Fig. 4. Fig. 3 shows the variation of $\bar{\sigma}_r$ in the vessel while Fig. 4 shows $\bar{\sigma}_\theta$. Dots represent the results of the numerical solution by Chen and Lin.

Next, a spherical pressure vessel of wall thickness $a/b = 0.5$ subjected to external pressure is considered. The results of the calculations for this case are plotted in Fig. 5 and Fig. 6. As before dots in these figures come from the numerical solution of Chen and Lin [1]. The distribution of $\bar{\sigma}_r$ and $\bar{\sigma}_\theta$ for different values of β can be visualized in these figures, respectively.

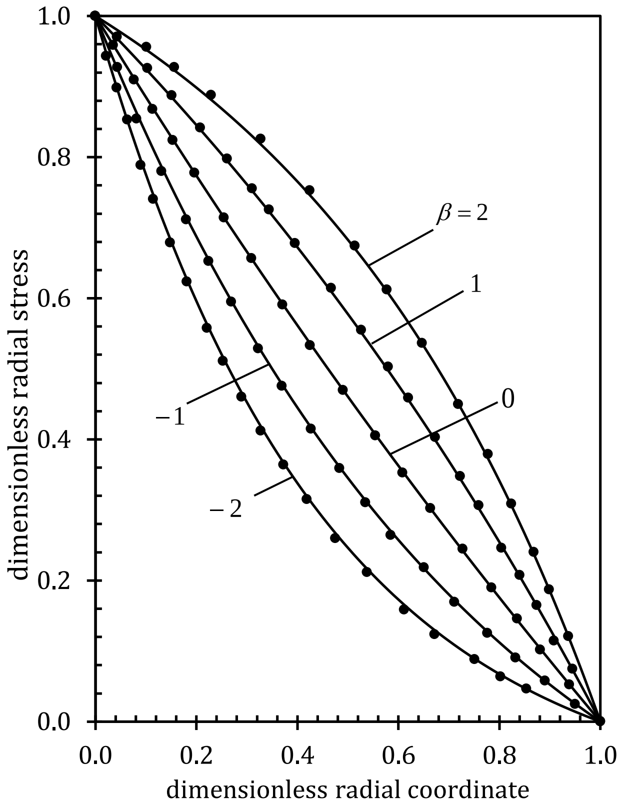

Figure 1. Variation of dimensionless radial stress in a cylindrical pressure vessel of *a/b* = 0.9 subjected to internal pressure for different values of *β*.

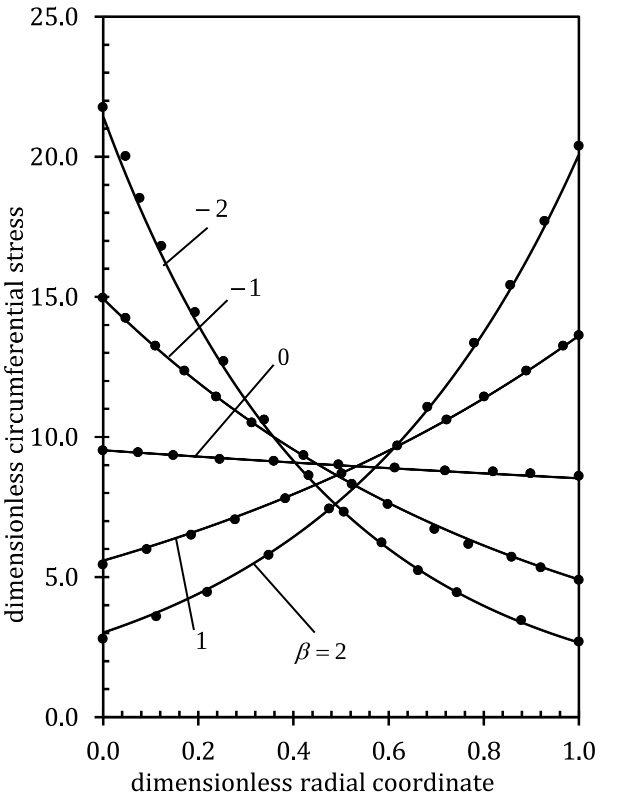

Figure 2. Variation of dimensionless circumferential stress in a cylindrical pressure vessel of *a/b* = 0.9 subjected to internal pressure for different values of *β*.

Journal of Multidisciplinary Engineering Science and Technology (JMEST)
ISSN: 3159-0040
Vol. 2 Issue 10, October - 2015

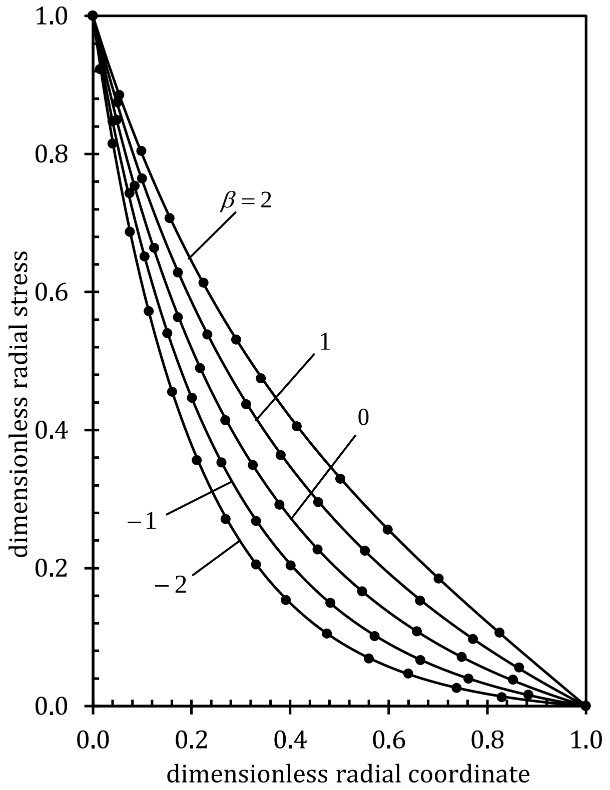

Figure 3. Variation of dimensionless radial stress in a spherical pressure vessel of *a/b* = 0.5 subjected to internal pressure for different values of β.

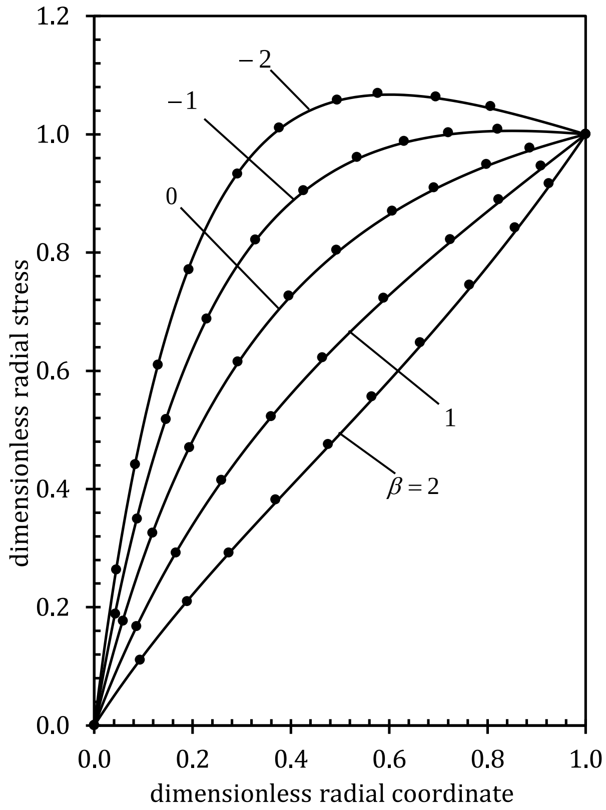

Figure 5. Variation of dimensionless radial stress in a spherical pressure vessel of *a/b* = 0.5 subjected to external pressure for different values of β.

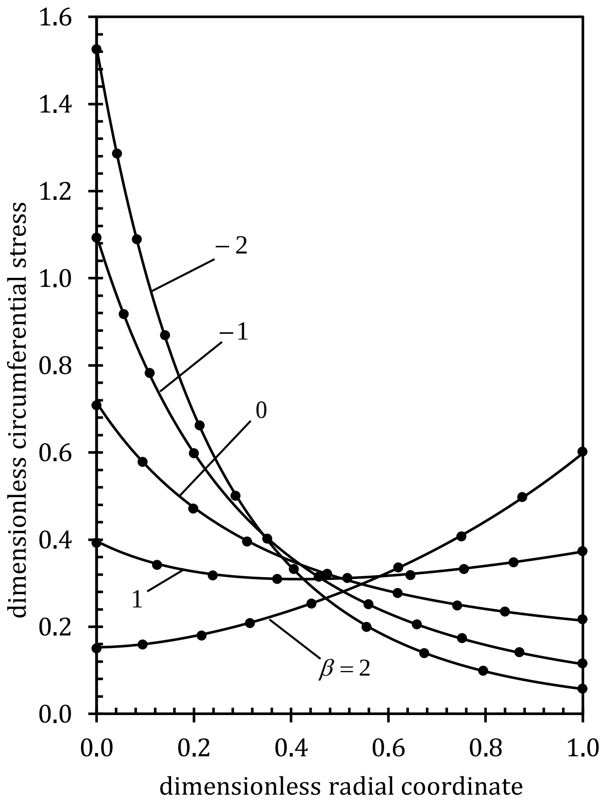

Figure 4. Variation of dimensionless circumferential stress in a spherical pressure vessel of *a/b* = 0.5 subjected to internal pressure for different values of β.

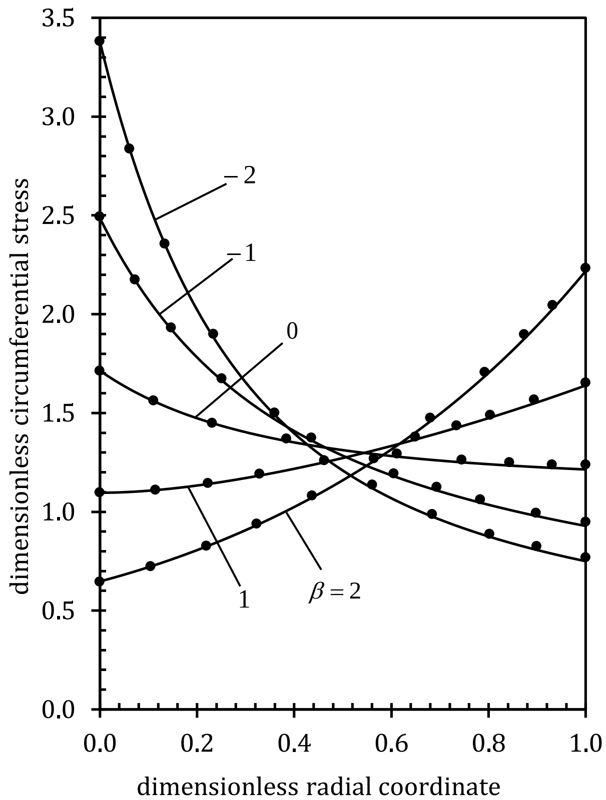

Figure 6. Variation of dimensionless circumferential stress in a spherical pressure vessel of *a/b* = 0.5 subjected to external pressure for different values of β.

Table 1. $\bar{\sigma}_r$ vs r for $a/b = 0.5$ using β as a parameter. Analytical and numerical [1] results.

	$\bar{\sigma}_r$ for $\beta=-2$		$\bar{\sigma}_r$ for $\beta=-1$		$\bar{\sigma}_r$ for $\beta=0$		$\bar{\sigma}_r$ for $\beta=1$		$\bar{\sigma}_r$ for $\beta=2$	
$\bar{r}$	Analytical	Numerical	Analytical	Numerical	Analytical	Numerical	Analytical	Numerical	Analytical	Numerical
0.0	1.0000000	1.000	1.0000000	1.000	1.0000000	1.000	1.0000000	1.000	1.0000000	1.000
0.1	0.6505686	0.651	0.7105925	0.711	0.7685950	0.769	0.8202738	0.820	0.8619429	0.862
0.2	0.4276402	0.428	0.5083599	0.508	0.5925926	0.593	0.6731116	0.673	0.7423432	0.742
0.3	0.2823479	0.282	0.3639224	0.364	0.4556213	0.456	0.5495138	0.550	0.6355641	0.636
0.4	0.1859609	0.186	0.2588679	0.259	0.3469388	0.347	0.4433901	0.443	0.5375866	0.538
0.5	0.1210635	0.121	0.1812791	0.181	0.2592593	0.259	0.3504783	0.350	0.4454018	0.445
0.6	0.0768235	0.077	0.1232281	0.123	0.1875000	0.188	0.2677075	0.268	0.3566439	0.357
0.7	0.0463535	0.046	0.0793152	0.079	0.1280277	0.128	0.1928075	0.193	0.2693578	0.269
0.8	0.0251905	0.025	0.0457863	0.046	0.0781893	0.078	0.1240609	0.124	0.1818444	0.182
0.9	0.0103944	0.010	0.0199848	0.020	0.0360111	0.036	0.0601404	0.060	0.0925526	0.093
1.0	0.0000000	0.000	0.0000000	0.000	0.0000000	0.000	0.0000000	0.000	0.0000000	0.000

Table 2. $\bar{\sigma}_\theta$ vs r for $a/b = 0.5$ using β as a parameter. Analytical and numerical [1] results.

	$\bar{\sigma}_\theta$ for $\beta=-2$		$\bar{\sigma}_\theta$ for $\beta=-1$		$\bar{\sigma}_\theta$ for $\beta=0$		$\bar{\sigma}_\theta$ for $\beta=1$		$\bar{\sigma}_\theta$ for $\beta=2$	
$\bar{r}$	Analytical	Numerical	Analytical	Numerical	Analytical	Numerical	Analytical	Numerical	Analytical	Numerical
0.0	3.3699069	3.370	2.4699608	2.470	1.6666667	1.667	1.0007634	1.001	0.4975766	0.498
0.1	2.3821340	2.382	1.9259313	1.926	1.4352617	1.435	0.9576049	0.958	0.5428856	0.543
0.2	1.7087768	1.709	1.5262081	1.526	1.2592593	1.259	0.9369132	0.937	0.6065827	0.607
0.3	1.2412574	1.241	1.2263143	1.226	1.1222880	1.122	0.9328087	0.933	0.6879382	0.688
0.4	0.9116622	0.912	0.9973463	0.997	1.0136054	1.014	0.9415295	0.942	0.7874116	0.787
0.5	0.6762864	0.676	0.8199113	0.820	0.9259259	0.926	0.9606168	0.961	0.9063597	0.906
0.6	0.5063291	0.506	0.6806403	0.681	0.8541667	0.854	0.9884465	0.988	1.0469030	1.047
0.7	0.3824267	0.382	0.5701008	0.570	0.7946943	0.795	1.0239492	1.024	1.2118854	1.212
0.8	0.2913360	0.291	0.4815027	0.482	0.7448560	0.745	1.0664364	1.066	1.4048932	1.405
0.9	0.2238652	0.224	0.4098711	0.410	0.7026777	0.703	1.1154907	1.115	1.6303192	1.630
1.0	0.1735525	0.174	0.3515051	0.352	0.6666667	0.667	1.1708939	1.171	1.8934617	1.893

APPENDIX

Analytical Solution to Annular Disk

For a stationary (non-rotating) annular disk of inner radius a, outer radius b the two basic equations are those given by (2) and (3). In a state of plane stress, $\sigma_z = 0$, hence the equations of the generalized Hooke's law read

$$\epsilon_r = \frac{1}{E}[\sigma_r - \nu\sigma_\theta], \tag{47}$$

$$\epsilon_\theta = \frac{1}{E}[\sigma_\theta - \nu\sigma_r]. \tag{48}$$

where E has been defined by (1). Using a stress function as in (9), the elastic strains can be put into the forms

$$\epsilon_r = \frac{1}{E}\left[\frac{F}{r} - \nu\frac{dF}{dr}\right], \tag{49}$$

$$\epsilon_\theta = \frac{1}{E}\left[\frac{dF}{dr} - \nu\frac{F}{r}\right]. \tag{50}$$

Substitution of elastic strains into the compatibility relation, (3), leads to the governing differential equation for disk geometry

$$\frac{d^2F}{dr^2} + \left(\frac{1}{r} - \frac{\beta}{b-a}\right)\frac{dF}{dr} - \left(\frac{1}{r} - \frac{\beta\nu}{b-a}\right)\frac{F}{r} = 0. \tag{51}$$

The general solution is

$$F(r) = C_1P(r) + C_2Q(r)\,, \tag{52}$$

where

$$P(r) = r\left[1 + \frac{\beta(1-\nu)}{3(b-a)}r + \frac{\beta^2(1-\nu)(2-\nu)}{24(b-a)^2}r^2\right.$$
$$+\frac{\beta^3(1-\nu)(2-\nu)(3-\nu)}{360(b-a)^3}r^3$$
$$+\frac{\beta^4(1-\nu)(2-\nu)(3-\nu)(4-\nu)}{8640(b-a)^4}r^4$$
$$+\frac{\beta^5(1-\nu)(2-\nu)(3-\nu)(4-\nu)(5-\nu)}{302400(b-a)^5}r^5$$

$$+\frac{\beta^6(1-\nu)(2-\nu)(3-\nu)(4-\nu)(5-\nu)(6-\nu)}{14515200(b-a)^6}r^6 + \cdots \Bigg], \tag{53}$$

and

$$Q(r) = P(r)\int_a^r \exp\left(\frac{\beta\lambda}{b-a}\right)\frac{d\lambda}{\lambda P(\lambda)^2}\ . \tag{54}$$

References

[1] Chen, Y.Z. and Lin, X.Y., Elastic analysis for thick cylinders and spherical pressure vessels made of functionally graded materials. Computational Materials Science Vol. 44, pp. 581-587, 2008.

[2] Timoshenko, S. and Goodier, J.N., Theory of Elasticity, 3rd ed., McGraw-Hill, New York, 1970.

[3] Eraslan, A.N. and Akis, T., On the plane strain and plane stress solutions of functionally graded rotating solid shaft and solid disk problems. Acta Mechanica Vol. 181, pp. 43-63, 2006.

[4] Eraslan, A.N., Apatay, T. and Gulgec, M., Elastic-plastic stress analysis of nonhomogeneous rotating solid discs. (in Turkish) Journal of Faculty of Engineering and Architecture of Gazi University Vol. 23, pp. 627-635, 2008.

[5] Nie, G.J. and Batra, R.C., Stress analysis and material tailoring in isotropic linear thermoelastic incompressible functionally graded rotating disks of variable thickness. Composite Structures Vol. 92, pp. 720-729, 2010.

[6] Peng, X.L. and Li, X.F., Thermoelastic analysis of a cylindrical vessel of functionally graded materials. International Journal of Pressure Vessels and Piping Vol. 87, pp. 203-210, 2010.

[7] Akbarzadeh, A.H., Zad, S.K.H., Eslami, M.R. and Sadighi, M., Mechanical behavior of functionally graded plates under static and dynamic loading. Proceedings of the Institution of Mechanical Engineers Part C-Journal of Mechanical Engineering Science Vol. 225, pp. 326-333, 2011.

[8] Iaccarino, G.L. and Batra, R.C., Analytical solution for radial deformations of functionally graded isotropic and incompressible second-order elastic hollow spheres. Journal of Elasticity Vol. 107, pp. 179-197, 2012.

[9] Fallah, F. and Nosier, A., Nonlinear behavior of functionally graded circular plates with various boundary supports under asymmetric thermo-mechanical loading. Composite Structures Vol. 94, pp. 2834-2850, 2012.

[10] Ghannad, M., Nejad, M.Z., Rahimi, G.H. and Sabouri, H., Elastic analysis of pressurized thick truncated conical shells made of functionally graded materials. Structural Engineering and Mechanics Vol. 43, pp. 105-126, 2012.

[11] Zozulya, V.V. and Zhang, C., A high order theory for functionally graded axisymmetric cylindrical shells. International Journal of Mechanical Sciences Vol. 60, pp. 12-22, 2012.

[12] Nejad, M.Z., Abedi, M., Lotfian, M.H. and Ghannad, M., An exact solution for stresses and displacements of pressurized FGM thick-walled spherical shells with exponential-varying properties. Journal of Mechanical Science and Technology Vol. 26, pp. 4081-4087, 2012.

[13] Argeso, H., Analytical solutions to variable thickness and variable material property rotating disks for a new three-parameter variation function. Mechanics Based Design of Structures and Machines Vol. 40, pp. 133-152, 2012.

[14] Kim, J. and Reddy, J.N., Analytical solutions for bending, vibration, and buckling of FGM plates using a couple stress-based third-order theory. Composite Structures Vol. 103, pp. 86-98, 2013.

[15] Alibeigloo, A., Three-dimensional semi-analytical thermo-elasticity solution for a functionally graded solid and an annular circular plate. Journal of Thermal Stresses Vol. 35, pp. 653-676, 2012.

[16] Arslan, E. and Eraslan, A.N., Bending of graded curved bars at elastic limits and beyond. International Journal of Solids and Structures Vol. 50, pp. 806-814, 2013.

[17] Tutuncu, N. and Temel, B., An efficient unified method for thermoelastic analysis of functionally graded rotating disks of variable thickness. Mechanics of Advanced Materials and Structures Vol. 20, pp. 38-46, 2013.